JAST, Vol. 12, No. 1, pp. 1- 13

JAST
Journal of Aerospace Science and Technology

Experimental and Numerical Investigation of Unsteady Flow around Cylinder with Four Plates Perpendicular to it with Rotational Degree of Freedom

H. Isvand[1], A. Sharafi[2]* and A. Salmaninejad

1, 2, 3.Dept. of Aerospace Eng. ShahidSattari Aeronautical Univ. of Science and Technology,

*Tehran, IRAN

sharafi@ssau.ac.ir

In this study, the behavior of a subject consisting of a cylinder with four plates perpendicular to it with a rotational degree of freedom under airflow both through the numerical approach, known as improved discrete vortex and experimental approach were investigated. The experimental and numerical results have shown that oscillating regime occurs in low velocity and length. This movement is vibrations with irregular range around an equilibrium angle of 45 degrees. In oscillating motion regime, it is seen that after releasing the object in free flow, a high torque force, due to the flow acceleration from the model, is induced to the plates and makes a big angular change, but after a while, the range of oscillation around the equilibrium angle of 45 degrees decreases. The probability of rotational motion regime in length ratio of one and velocity of 13 m/sec in initial angle of attack is low. However, the experimental and numerical results have indicated that still in high initial angle of attack around 45 degrees, owing to the induced decreased torque to plates, there exists an oscillating movement. Rotational regime in length ratio of 3 and free flow velocity of 13 m/sec is observedin all initial angle of attack. In addition, rotational regime appears in all initial angle of attack with the length ratio of 4 and different free flow velocities because of increase in the area of plates.

Keywords: Unsteady flow; Vortex Panel Method; Rotational and vibrational motion; Forced vibration; Wind tunnel tests

Nomenclature

c	chord
$\boldsymbol{h}$	local thickness of the body
$\boldsymbol{J_*}$	non-dimensional inertia moment
$\boldsymbol{L/R}$	length ratio
M_{Z_*}	non-dimensional aerodynamic moment induced on the plate
$\boldsymbol{n_c}$	number of divisions on the cylinder
$\boldsymbol{n_k}$	number of divisions on the plates
$\boldsymbol{n_p}$	number of the plates attached to the cylinder
$\boldsymbol{n_V}$	vector perpendicular to the surface
$\boldsymbol{R_e}$	Reynolds number
$\boldsymbol{r_*}$ a	local non dimensional coordinate and along the bodylength
$\boldsymbol{r_c}$	radius of discrete zone
$\boldsymbol{\Delta r}$	distance between two neighboring stuck
$\boldsymbol{S_t}$	Strouhal number
$\boldsymbol{R_e}$	Reynolds number
$\boldsymbol{\Gamma}$	strength of released vortices from the flow
ρ	free flow density
$\boldsymbol{\rho_{t^*}}$	non-dimensional density of the body
$\boldsymbol{\delta}$	strength of the vortices attached to the body
$\boldsymbol{\delta_{0i}}$	strength of vortex$i$
r_*a	local non dimensional coordinate and along the body's length

1. Assistant Professor
2. Lecturer(Corresponding Author)
3. M. Sc. Graduate

φ	angle between free velocity and semi-plate indicator
φ_0	initial body angle of attack strength of the vortices attached to the body

Introduction

In the nature, the influence of a fluid flow with a solid object results in a force on the surface of an object. If the object is flexible, this force leads to a change in the object shape; otherwise, if the object is solid, this force moves the object from its position to a new one, in proportion with the amount of the force. In return, the reactional force from the solid object surface causes a shape change in the flow pattern. This mechanism causes any mirror attentions in the flow variables result in proportional changes in other dynamic variables.

Many years ago, the vortex trial mechanism around the wake behind objects was first investigated by Von Karman. This research was initiated and developed based upon the induced vibrations by vortices. He reported his analyses based on the numerical approaches in the wake behind the object, the lift and drag forces induced on the objects and flow separation. In the early 1940s, some observations from objects responses to the vibrations stemmed from liberating forces of vortices were published. When an object is put in fluid flow, flow separation from its surface occurs. Flow separation results in change from a steady to an unsteady one with increase in Reynolds number. In low Reynolds number, the surrounded flow around the object is steady. When the first flow separation occurs, the Reynolds number increases and reaches a definite value, unsteadiness in the shear layers appear and develop in the separated flow. So, nonlinear interferences between the layers of flow and return flow from the wake were subsequently formed, leading to Von Karman Vortex Street behind the object. Vortices in two opposite directions are arranged in a way that these vortices and turbulent flow area are behind the cylinder [1].

In the fields of contemporary aerospace technology, studying and investigating the unsteady flow around objects and rotational/ oscillating plates (antennas, Gigs, etc.) areof high importance to provide the performance requirements of these devices.It is necessary to meticulously observe their behaviors under varying degrees of freedom with numerous geometric characteristics, and their directions in the flow of these characteristics, formation and distributionof the vortices resulting from flow separation from sharp edges and the loss ofsteadiness of vortex layers. Vortex induced vibration (VIV) is a phenomenon that is created by the clash between fluid flow and the structure behind a solid object. This phenomenon is also applicable in tall buildings, power lines and oil extraction pipes from the sea. To put it simply, when an ever flow passes by an object, it starts to make turbulence; and well-arranged vortices behind objects are created. In case of an irregular arrangement, an oscillating lifting force on the object and its fluctuation are produced. Non-permanent flow is made both spontaneously and obligatorily. But, in the spontaneous state, non-permanent flow is created resulting from the increase of unsteadiness in the fluid or absence of initial. In contrast, obligatory non-permanent flow is created as a result of boundary layers and the sources moving in the flow. The VIV emerged as a result of the nonlinear interference of the object with the wake, has attracted much attention from experts in different engineering fields.

Many people have theoretically, experimentally and semi-experimentally studied this field. There are mainly two experimental approaches to investigating this issue: (1) Free vibration and(2) Forced Vibration.

In the free vibration approach, the process is often carried out in a wind/ water tunnel along with other external mechanisms. The structure or the object under study is supported via springs, dampers or any other elastic systems. Concerning the nature of vortices release toward the downstream, this study aims to find out the variables that emerge during his time in the form of vibrations and oscillation.

Fengs (1968) conducted some studies on the cylinder under free vibration in wind tunnel [2]. In these experiments, the cylinder was attached to the body of the object via a tensional spring [2]. Amandoles (2010) performed similar studies on a cylinder with a square cross section in wind tunnel [3]. Umemuraetal. (1971) observed that the aerodynamic damping factor for a cylinder under free vibration is in the form of a negative damping force for the Strouhal number of 0.2[4]. They have found out that the vibrational or oscillating indicators (variables) for a cylinder merge just when the damping force is a negative value. So, it creates an extra condition for a self-excited motion. Despite the fact that Sarpkaya (1978, 2004) proposed an opposite view about self-excited vibrations, they

declared that self-excited vibration results from the vortex release that is liberated from the object towards the downstream. In other words, objects never excite themselves. Additionally, there is an alternating force that arises for keeping or controlling the object motion.

When the object stops moving, this alternating force disappears. This definition is in sharp contrast with a solid object vibration. Because for a solid object there is no motion, but there still exists an alternating lifting force. Sarpkaya has stated that in case of lock-in, the frequency of vortex release and object vibrations approach a unified frequency [6]. The characteristics of self-excited objects, proposed by Umemura could attract Scalan and Rosenbaum's attention in 1968[7]. They maintained that there are some forces that produce extra energy in the system (fluid flow and object) that may be interpreted as negative damping. In case of negative damping, energy needs to be transferred. But for a system with a positive damping, the damping force performs the negative work. However, for a negative damping, the damping force does the positive work on the system which needs energy transfer [7]. Protoset al. (1968) could calculate the transferred energy from a fluid flow to a self-excited cylinder. Bearman and Obasaju (1982) conducted a meta-analysis on the cylinders (square crosssection) fixed in forced vibrations. They have indicated that the vibrational lifting coefficient for a cylinder (square crosssection) in the area of simultaneous frequency is much less than rotating cylinder (circle crosssection) under the same experimental conditions. Furthermore, in low velocities, vortex release may disappear. Before the lock-in or synchronize area, the forced vibrations of the cylinder dominate its motion and the vibration of vortex release disappears. Also, Bearman (1984) restarted the object vibrations resulted from vortex shedding from its surface [9]. Williamson and Roshko (1988) outlined a mechanism for determining the location, shape and from of the vortices shed from the flow. As it can be seen in Fig. 1, a particular pattern about vortex shedding in the wake, resulting from motion, is created [10]. These patterns consist of 2S mode (two separate vortices in each cycle) and 2P mode (two pairs of vortices in each cycle). If forced vibrations are induced to the object, another mode from vortex shedding named P+S mode (one discrete vortex and a pair of vortices in each cycle) may appear. 2S, 2P and P+S modes in Fig. 1 can be seen near synchronization frequency [10]. Griffin (1976) indicated that 2P and P+S modes control object vibrations and oscillation.

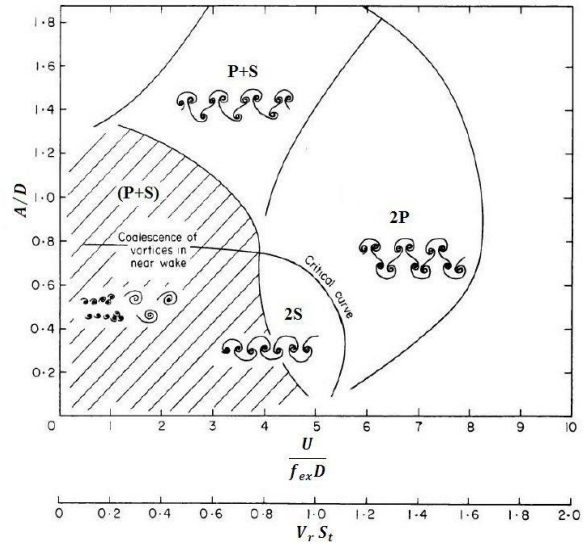

Fig. 1 Map of vortex patterns [10].

This study investigates the behavior of a cylinder with 4 plates perpendicular to it with rotational degree of freedom in airflow. Due to the bidirectional effects of airflow and cylinder with the rotating plates as well as the flow unsteadiness, there is no appropriate analytical procedure to solve it. Therefore, discrete vortex approach was employed to calculate the vertical force coefficient and the torque from aeronautical forces. Also, modeling was performed during free rotation. Some experiments on the cylinder with 4 plates with the rotational degree of freedom in wind tunnel were carried out and the dynamic behaviors of the model concerning the changes in the parameters namely length ratio (L/R), free flow velocity and different initial angle of attacks (φ_0) were investigated.

Statement of Problem and Numerical Approach

Due to the effects of free flow on the object(a cylinder with 4-plates attached to it) and the bidirectional effects of the moving object on the flow, there is virtually no appropriate analytical procedure to solve the problem. Furthermore, the flow is to a great extent unsteady, so, solving such a problem using simple numerical modeling procedure based on Navier- Stoke's equation and

Reynolds number is too difficult. As a result, vortex panel method was utilized for this problem(Fig. 2).

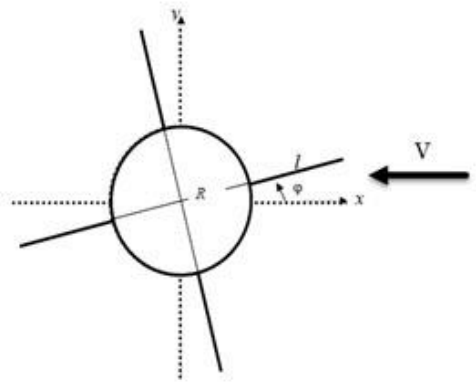

Fig. 2 Schematic of the studied object and its geometric parameters

This method was founded on Helmholtz theorem. According this theorem, vortex in deal flow always moves with material particles. If vortex distribution is calculated; consequently, velocity domain, which is the sum of induced velocities of all vortices, is obtained. In discrete vortex approach, the body surface is replaced by a vortex layer and the vortices attached to the body, free vortices(regarding place and time) and boundary layers get discreticized, the attached vortices move with the body,whiletheir strength depends on the time and is calculated by impenetratability condition in controlling points. Free vortices move with the flow and their strength in ideal flow is regarded fixed. According to Helmholt's theorem, this is generally a result of clash with the solid body. It is also worth mentioning that in the absence of a solid boundaryin a viscous flow, regardless of vortex dissipation, the total amount of strength remain fixed. Therfore, in case of vortex separation in the viscous flow, there exists the probability of dissipation and vortex strength reduction. At each step, a free vortex from sharp edges(due to flow separation) releases by passage. The number of free vortices increases Biot-Savart law was employed to claculate the induced velocity from the vortex. Based upon this law, the induced velocity in the center of vortex approaches infinity. As distance from the center increases, the velocity decreases. Hence, when the singularity point is in the center, it needs tobe solved which can be doneby discrete zone procedure. In this procedure, a zone with the radius (r_c) around the center of the vortex is regarded(discrete zone) in which the velocity changes from zero(in the circle center) to the maximum(on the circle layer). Out of this zone(without discontinuity in the boundary), Biot-Savart law is used. In this case, the velocity domain meets countiniuty equation and Coushy problem, even in case of unsteadiness, it is suitable for vortices movement.

The parameter $r_c$is named the radius of discrete zone and is calculated as:

$$V_\theta = \frac{\Gamma}{2\pi r} : r > r_c \, , V_\theta = \frac{\Gamma}{2\pi r}\frac{r}{{r_c}^2} : r < r_c V_r = 0 \quad (1)$$

Put coordinate(x, y) in the center of cylinder(Fig.3) as $x$is in the direction of the flow. Incompressibility condition of the flow in a non-directional state isas follows:

$$\left|\overline{div V_*}\right| = 0 \quad (2)$$

The compressible flow movement equation (without inducing the bouncy) in non-dimensional form is as follows:

$$\frac{d\vec{V}_*}{dt_*} = -\nabla_*(p_*) + \frac{1}{Re}\Delta_*\vec{V}_* \quad (3)$$

Assume thatr_* is a local non-dimensional coordinate and along the body length. So, the equation of free rotation is as follows:

$$J_*\ddot{\varphi} = M_{Z_*} = \int_{-1}^{1} r_*\Delta p_*(r_*)dr_* \quad (4)$$

$\varphi$is the angle between velocity of free flow and semi-plate indicator M_{Z_*} is the non-dimensional aerodynamic moment induced on the plate:

$$M_{Z_*} = \frac{2M_Z}{L^2\rho U^2} \quad (5)$$

$J_*$is the non-dimensional inertia moment:

$$J_* = \int_{-1}^{1} \rho_{t^*}(r_*){r_*}^2\, dr_* \quad (6)$$

$\rho_{t^*}$is non-dimensional density of the body:

$$\rho_{t^*}(r_*) = \frac{\rho_w h(r_*)}{\rho L} \quad (7)$$

$h$is the local thickness of the body,ρ_w the density andρas the free flow density.

To determine the total amount of the vortices attached and released in different times, the impenetrability condition was used. The boundary condition of impenetrability is as follows:

$$\left(\vec{V}\cdot\overrightarrow{n_V}\right)=|r_*|\dot{\varphi} \tag{8}$$

In which n_V is the vector perpendicular to the surface. To calculate the effects of free vortex dissipation, the semi-experimental vortex loss procedure is used. So, the strength of vortex i; depends on time.

$$\delta_i(t)=\delta_{0i}\left\{1-e^{\left[\frac{-k}{4(t-t_{0i})}\right]}\right\} \tag{9}$$

In which $\delta_{0i}$of isthe strength of vortex$i$ in its birth, k an experimental value as a dissipation indicator,t_{0i} the birth of vortex$i$and the optimum value of k is 40[12]. The initial requirement of the problem is as follows:

$$\forall(x,y),t=0\ \rightarrow v=0\ ,u=0 \tag{10}$$

Also, the thickness of cylinder and plates is considered zero and $*$ is used for simplification. When $t=0$ then, the velocity of equation is as follows:

$$v_\infty=0\ ;\ u_\infty=u_\infty(t) \tag{11}$$

In free rotational state, to avoid a sudden force on the surface, the no dimensional velocity change from zero to maximum is one:

$$u_\infty(t)=1-(1-t)^2 \tag{12}$$

The angle of plate indicator with the free flow is called φ (Fig.3), and the initial angular velocity of the plate ($\dot{\varphi}$) is regarded zero. The other extra requirement for solving unsteady flow is Kelvin's condition. This condition states that the total amount of vortices during time remains constant and equal to zero, so:

$$\sum_{i=1}^{n}\Gamma_i+\sum_{i=1}^{m}\delta_i=0 \tag{13}$$

In which n represents the attached vortices of the body,m accounts for the free vortices, δ and$\Gamma_i$represent the strength of the vortices attached to the body and the strength of released vortices from the flow, respectively.

To determine the strength of the attached vortices and each vortex released from edges, the condition of impenetrability in controlling point (formula 8) is used. Controlling points locate in the middle distance of attached vortices and on edges.

As a result, at each time, an algebraic coordinate consisting of $n_c+n_p\times n_k+1(n_c$ represents the number of divisions on the cylinder, $n_p$as the number of the plates attached to the cylinder and $n_k$represents the number of divisions on the plates) and $n_c+n_p\times n_k$ (passive) is obtained. As can be seen, in an indefinite coordinate system, we have put a source with a strength near zero in the center of cylinder. To solve it, we have employed gauss elimination. After obtaining the strength of stuck vortices, the induced velocity resulting from all free and stuck vortices on released vortices in current time step and vortices free in the atmosphere needs to be calculated. To determine the velocity in the initial coordinate system, it is necessary to addthe velocity of all the free and stuck vortices with that of the free flow. So, velocity at the location with the coordinates of r is as follows:

$$u(\vec{r})=\sum_{i=1}^{n}\Gamma_i u_i(\vec{r})+\sum_{l=1}^{m}\delta_l u_l(\vec{r})+u_\infty(t) \tag{14}$$

$$v(\vec{r})=\sum_{i=1}^{n}\Gamma_i v_i(\vec{r})+\sum_{l=1}^{m}\delta_l v_l(\vec{r}) \tag{15}$$

To locate the free vortices at next time steps, the motion equation of each vortex, using Euler's method, is integrated.

$$\vec{r}_{j+1}^{n+1}=\vec{r}_j^{n}+\vec{V}^n\left(\vec{r}_j^{n}\right)\Delta t \qquad j=1\ ,m \tag{16}$$

Here,$\vec{r}_j^{n}=\left(x_j^n;y_j^n\right)$ represents the current time step, Δtas the time step and $j$represents the numbers of free vortices that it increases where each vortex is released. Given the overall induced velocity of inertial coordinate system, the body behavior at the next time step needs to be analyzed. Therefore, the induced velocity on all controlling points requires to be calculated, following that, pressure loss at the controlling point must be obtained.

$$\Delta p_i^m=\left(u_i^m\cos\varphi_m+v_i^m\sin\varphi_m\right)\frac{\Gamma_i^m+\Gamma_{i-1}^m}{2}\frac{1}{\Delta r}-\frac{\delta_l^m+\sum_{k=i}^{n}\left(\Gamma_k^m-\Gamma_k^{mp}\right)}{\Delta t} \tag{17}$$

In whichu_i^m and v_i^m are the velocity variables in direction of x, $y$at is the controlling points of i on the plate m, Γ_i^m is the strength of stuck vortex i, δ_l^mAs the strength of free vortex created from the plate $m$at the current time step,Γ_k^{mp}as the strength of stuck vortex k on plate $m$at the previous time step, $\varphi_m$as the angle between plate $m$and the vector of free velocity, and Δras is the distance between two neighboring stuck vortices. Equation (17) was obtained via Cauchy-Lagrange integration. The free rotation equation is as follows:

$$\dot{\varphi}_{n+1} = \dot{\varphi}_n + \ddot{\varphi}_n \Delta t \quad (18)$$

Using this equation, we can calculate the non-dimensional rotational moment induced on the plates attached to the cylinder through numerical investigation. Given the rotational moment, the plate non-dimensional angular acceleration at the following time step is as follows:

$$\varphi_{n+1} = \varphi_n + \dot{\varphi}_n \Delta t \quad (19)$$

$n$represents the current time step, and $n + 1$as the following time step. A very important point is considering the body physique. If some vortices approach the plate and cylinder as such distance becomes less than that between controlling points, as a result of plate displacement (Equations 18 and 19) and vortices movement (Equation 16), these vortices, using reflection theory, get far from the cylinder and plate. This is done as a consequence of regulating the velocity domain around the plate with the purpose of nonphysical vortices elimination around the body [13].

The Equipment and Methodology of Experimental Test

Having carried out the numerical modeling of the cylinder with four plates with rotational degree of freedom, it is necessary to check the reliability of the findings via experimental tests. To do so, equipment such as wind/ water tunnel and other instruments and appliances are required to create the body rotational degree of freedom. The required equipment consists of models, subsonic wind tunnel and electronic protractor device. It was the mentioned that the experiments are conducted for free vibrations in the flow which is steady and the dynamic behavior of the body in the air flow is investigated.

All the tests were done in the wind tunnel existing in the aerodynamic laboratory of aerospace faculty. This is a subsonic closed circuit wind tunnel and its maximum velocity is 50 m/sec. The test section of this tunnel is circular with the diameter of 50 cm. The distance between two inlets is 1 m and the turbulence intensity is less than 0.1%.

The experimental models are two cylinders with the lengths of 16 and 24 cm and diameter of 10 cm. On the body of cylinders, there are some grooves with the thickness of 2 mm to attach the plates. The aluminum plates with the lengths of 16 and 24cm and thickness of 2mm are screwed from the inside. These plates have the widths of 5, 10, 15 and 20 cm. The angle between the attached plates to cylinder is 90 degrees. The electronic protractor devices must have the capability of holding the model with the rotational degree of freedom in the wind tunnel, and also transferring the body behavior (vibration and rotation), after a definite process and analysis, to the concepts. So, the devices have two electronic and mechanical sections. The mechanical section has the responsibility for holding the model with rotational degree of freedom and transferring the behavior, and the electronic section has the responsibility of converting the behavior, body displacement from mechanical to electronic and transferring data to the computer.

After installing the plates on the cylinder, the model is put on the electronic protractor devices as it is exposed to the wind tunnel. It needs mentioning that this device is equipped with a particular brake that can put the model in different initial angles of attack and fix it in the flow. Serial portal was employed to transfer the data from the test to the computer, and also LabVIEW Software was utilized to archive and analyze the data. This software uses a special graphic programming language that can read and record the data from the serial port. After running Labview, a signal initially for releasing the brake of iPhone, is transferred to the micro controller, then the model starts to move, and the movement changes at each time step is achieved and recorded. The time step in Labview is 0.1 sec. So, the result from different velocities (10, 15, 20, 25, and 30m/sec), angles of attack (0, 8, 16, 24, and 32 degrees) and length ratio (1, 2, 3, and 4) have been recorded.

ResultsandDiscussions

Results for Numerical Method

A program with FORTRAN programming language was designed to model the unsteady flow around the cylinder with four plates attached to it regarding the discrete vortex as mentioned before. The time step dedicated is 0.1 sec and the time is between 0 toward 50 seconds. The variable parameters consist of plate length to cylinder radius ratio (L / R) with (the values of 0.667, 1, 1.5, 2.33 and 4) and initial object angles of attack of the plate to free flow (φ_0) (for the four plates, it is between 0 and 45 degrees). Also, the inertia moment is J=2.5

Ultimately the result have deduced that (L / R) and (φ_0) indicated a different flow pattern. Overall, the object movement regime in the flow is divided into four types. Type 1 occurs when the body oscillates (vibrates) around equilibrium position (special angle) known as steady vibration. Type 2 is when the body starts to rotate after release, called steady rotation. Type 3 occurs when the body in the flow oscillates around the equilibrium position, after that it enters the rotational regime. To put it simply, it can be said that this movement comprises vibrations with rotation which are also known as unsteady vibrations. Type 4 occurs when the body initially starts to rotate, when it enters vibrational regime. In other words, this simultaneous vibration and rotation is known as unsteady rotational regime.

The result from the numerical method displays that vibrational movement regimes are always present at low (L / R) and free flow velocities. In vibrational movement regime, the movement is with vibrations of irregular range around the equilibrium angle of 45 degrees.

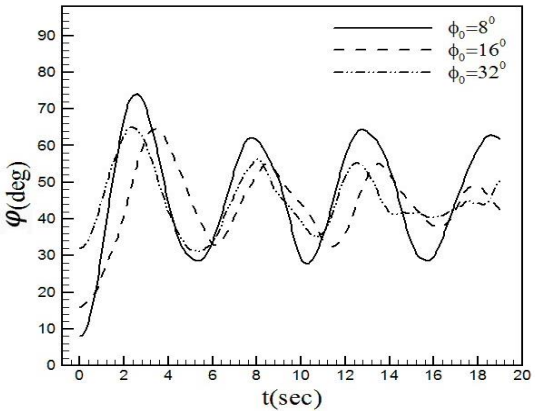

Fig. 3 Variation of object angle with time for length ratio 3 and free stream velocity6.3 m/sec

Figure 3 illustrates the angular changes respect to time for cylinder with four plates at free flow velocity (6.3m/sec) and ($L/R = 3$) at different initial angles of attack. The movement of the model in free flow in all initial object angles of attack around the angle of 45 degrees is vibrational. The model after release in the free flow and as a result of acceleration in free flow on the body, experiences angular changes. After some time, the range of vibrations around the body decreases to 45 degrees. Furthermore, it was observed that as the initial object angle of attack increases, the body vibrations range, resulting from the reduced torque induced to the plates, decreases. Rotational movement regime at $L/R = 1$ and velocity of 30m/sec at low initial object angle of attack was seen, but the movement around the high initial object angle of attack and around 45 degreeswasstill vibrational.

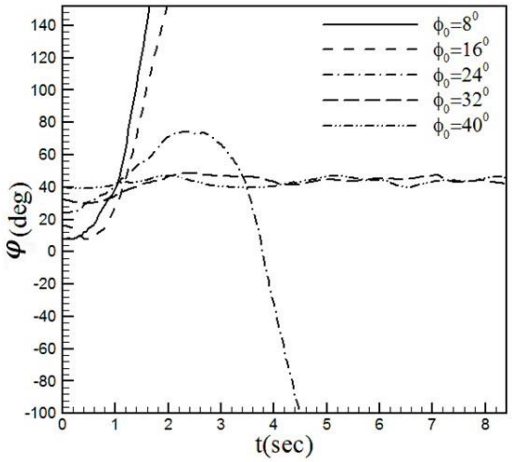

Fig. 4 Variation of object angle with time for length ratio of 2 and free stream velocity of 30 m/sec

Figure 4 illustrates this movement around $L/R = 2$ and velocity of 30 m/sec around different initial object angles of attack. It is crystal clear that the model tends to vibrate around the equilibrium angle of 45 degrees as the initial object angle of attack increases. Additionally, with initial object angle of attack increase in rotational movement regime, the angular velocity of the model decreases. In vibrational movement regime, the angular velocity of the model decreases as the initial object angle of attack decreases around 45 degrees. This can be attributed to the reduced torque induced to the plates. In$L/R = 4$, the movement regime at all initial object angles of attack and free stream velocity is seen as steady rotational. The more the initial object angle of attack approaches zero, the more the curve slope

increases and angular velocity of the body movement goes up.

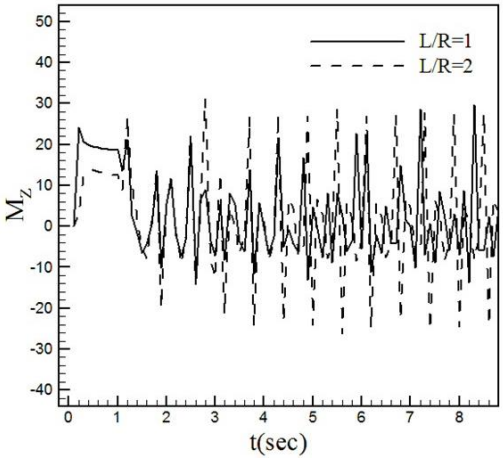

Fig. 5 Variation of moment coefficient with time for initial object angle of attack of 16 degrees and free stream velocity of 30 m/sec

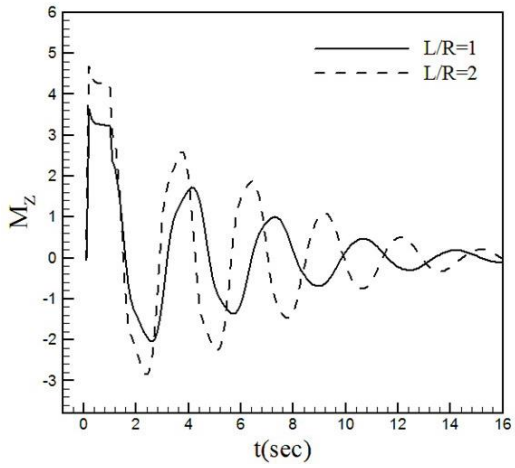

Fig. 6 Variation of moment coefficient with time for initial object angle of attack of 32 degrees and free stream velocity of 30 m/sec

Figure 5 and 6 illustrate the moment coefficient changes based upon time for rotational movement regime (initial object angle of attack is 16 degrees, and free stream velocity is 30m/sec) and vibrational movement regime (initial object angle of attack is 32 degrees and free stream velocity is 30m/sec) in$L/R = 1\,,2$. In rotational movement regime, the obtained moment irregularly changes with time, and the range of vibrations increases by time passage. But, in a vibrational movement regime, the moment coefficient changes with a sinusoidal vibration and different ranges during time. At the beginning of the model movement, a huge amount of moment is induced to the plates and the range of oscillation decreases by time passage. Also, in each oscillation, the moment and force which are approximately zero, near the equilibrium angle of 45 degrees, are induced to plates. In the both vibrational and rotational movement regimes, the increase of L/R leads to the maximum amount of moment coefficient. In other words, it can be stated that the amplitude of the moment oscillations induced to the plate increases which can be as a result of the plateL/R and surface area against airflow.

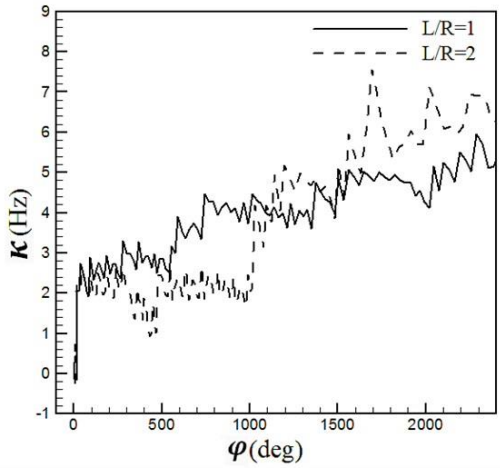

Fig. 7 Variation of dimming frequency with object angle for length ratio of 1, 2 and free flow velocity of 30 m/sec on initial object angle of 8 degrees

The dimming frequency (κ) is of important parameters of flow unsteadiness which is defined as$\kappa = \frac{\omega c}{2V}$. Here, $\omega$is the angular velocity of the model, c represents the longitudinal parameter and$V$represents isthe free stream velocity. Figure 7, illustrates the change of dimming frequency according to the angular changes for a cylinder with four plates (initial object angle of attack is 8 degrees and free stream velocity is 30 m/sec for rotational movement regime). When the body angular movement increases, the dimming frequency erratically and irregularly oscillates, and the amplitude of the dimming frequency in each rotation increases. From this time on, the average value of the dimming frequency remains fixed. The average value of dimming frequency, by L/R increase after time passage, increases as a result of model angular velocity. But it needs to be mentioned that at the beginning time, as the L/R increases, the dimming frequency decreases.

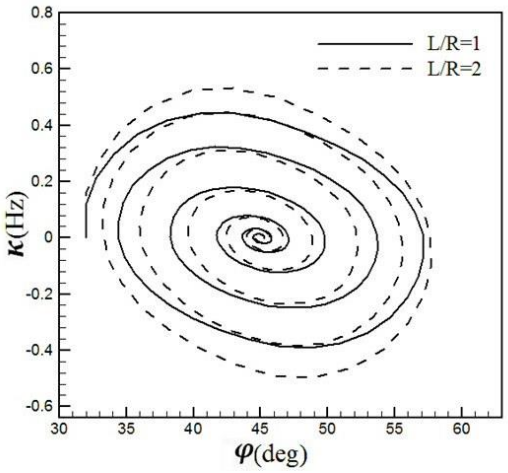

Fig. 8 Variation of dimming frequency with object angle for length ratio of 1, 2 and free flow velocity of 30m/sec on initial object angle of 32 degrees

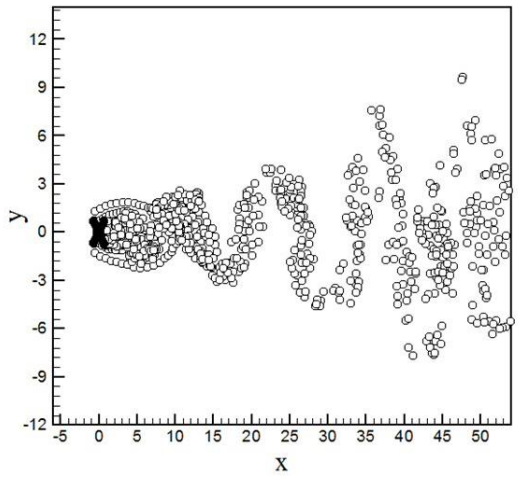

Fig. 9 Abandoned vortices distribution for length ratio of 2,initial object angle of attack of 32 degrees and free flow velocity of 10m/sec

Figure 8 illustrates the dimming frequency changes in proportion to angular changes in vibrational movement regime for a cylinder with four plates at the initial object angle of attack of 32 degrees and free stream velocity of 30m/sec. In each rotation, the dimming frequencyincreases along with angle increase. But, when the equilibrium object angle approaches 45 degrees, the dimming frequency reduces as a result of body angular velocity decrease; however, after exceeding this equilibrium angle, the dimming frequency once again goes up. As a consequence, some circles are made around the equilibrium angle of 45 degrees. When L/R increases, the amplitude of the dimming frequency increases in proportion with the model angular changes the behavior pattern still remains fixed. It is necessary to keep in mind that a change in the sign of dimming frequency represents the change of direction of the body.

Figure 9 indicates the disparity of the vortices released from the edges of the plates at the initial object angle of attack 32 degrees and free stream velocity of 10m/sec in $L/R = 2$ (vibrational movement regime) at the last time step. In the body vibrations around the equilibrium object angle of 45 degrees, vortices intermittently exit from the plates edges and enter free flow, and also create a particular in the wake behind the body. Regarding the identified and recognized patterns of vortex shedding towards the downstream determined by Williamson and Roshko, it is seen that the pattern of vortex shedding toward the downstream is as 2S. In other words, it is in the form of two vortices rotating in opposing directions in each vibration cycle. It needs to bear in mind that this pattern in rotational regime is irregular.

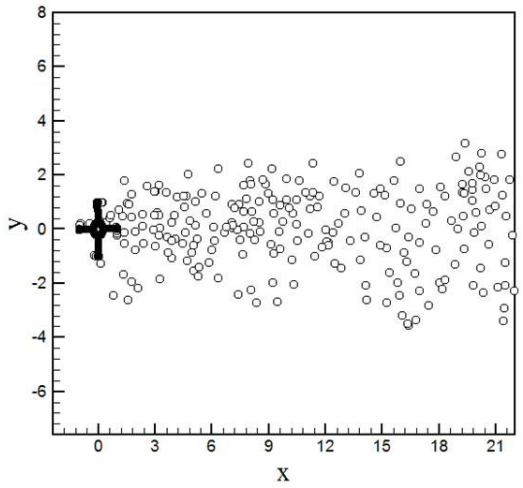

Fig. 10 Abandoned vortices distribution for length ratio of 3,initial object angle of attack of 8 degrees and free flow velocity of 15m/sec

Figure 10 shows itfor the initial object angle of attack of 8 degrees and free stream velocity of 15 m/sec in$L/R = 3$ at the last time step. This leads to further turbulences. Comparing the findings has revealed that body movement, in both rotational and vibrational movements, is as the result of vortices asymmetric distribution around the plates. In other words, it can be stated that the increase of vortex number for a plate leads to force reduction and ultimately moment decrease of that plate in comparison to another plate, creating vibrations or rotations around the body. But, in a vibrational movement regime, the vortex distribution around the equilibrium object

angle of 45 degrees is symmetric which reduces the force and moment induced to the plate, and finally leads to reduction in the body velocity at a particular angle.

Result obtained from experimental tests

Numerous experiments have been conducted on the cylinder with four plates in wind tunnel. The length of these cylinders were 16 and 24cm, respectively and L/R were equal to 1, 2, 3 and 4. Also, the experiments in the wind tunnel were carried out between 6 and 30m/sec under different initial body angles of attack (φ_0).

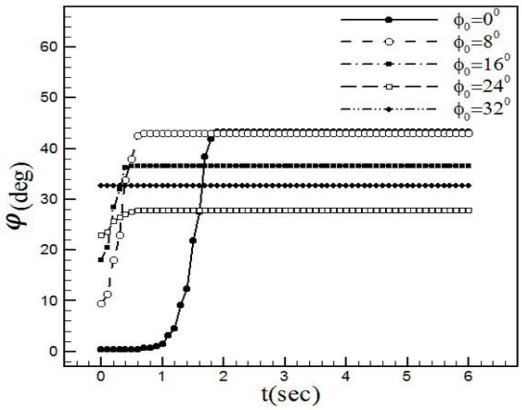

Fig. 11 Variation of object angle with time for cylinder with length of 16cm, length ratio of 1 and free stream velocity of 10m/sec

Figure 11 displays the model with the Reynolds number ranging from 1.32×10^5to9.92×10^6. In addition to studying the rotational, steady vibrational, unsteady rotational and unsteady vibrational, we also observed the damped movement around 45 degrees which almost occurs in low L/R and flow velocity. Figure 11 shows the angular changes of the cylinder with the length of 16cm during time and $L/R=1$ at free stream velocity of 10m/sec. As can be seen, when the body is released in the free flow, the body moves to the equilibrium angle of 45 degrees, then the movement is damped in the flow and finally remains fixed in the flow. As the flow velocity increases, Reynolds number also increases, the flow turbulences change the model behavior to damped and vibrational around 45 degrees. When the free velocity goes up, the other vibrations of the body in the free flow do not get damped, and the body constantly vibrates.

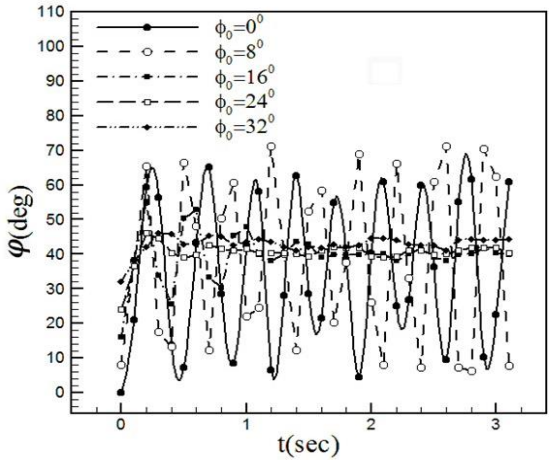

Fig. 12 Variation of object angle with time for cylinder with a length of 16cm, length ratio of 1 and free stream velocity of 30m/sec

This steady vibrational movement around the equilibrium angle of the cylinder with the length of 16cm, $L/R = 1$ and at 30m/sec can be seen in Fig. 12. This movement is in the form of steady vibration around the angle of 45 degrees. The vibrations amplitude is variable; the maximum amplitude for low initial object angle of attack is near zero which leads to a great amount of induced force to the plates at low initial object angle of attack.

Figure 13 indicates the boundary to convert the vibrational movement to rotational for a 16cm, $L/R = 2$ and free velocity of 15m/sec, and the cylinder of 24cm length, $L/R = 1$ and free velocity of 30m/sec. This stems from the effects of the flow with two dimensions.

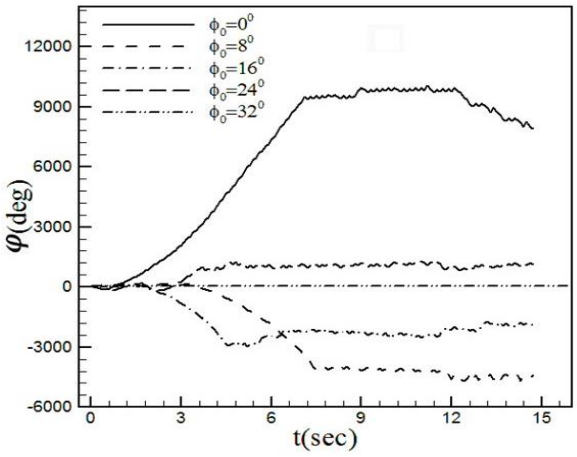

Fig. 13 Variation of object angle with time for cylinder with a length of 24cm, length ratio of 1 and free stream velocity of 30m/sec

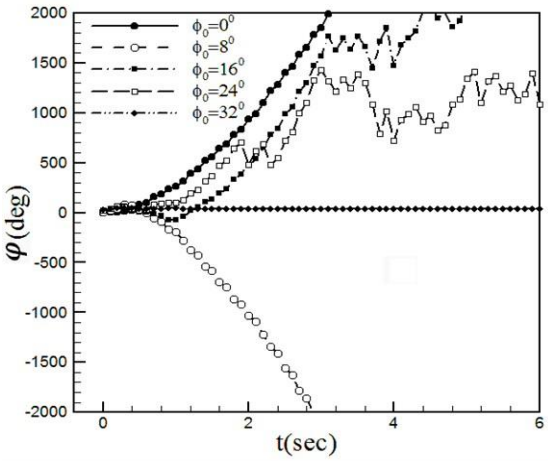

Fig. 14 Variation of object angle with time for cylinder with a length of 16cm, length ratio of 2 and free stream velocity of 20m/sec

Figure 14 illustrates the angular changes over time for a cylinder of 16cm length, $L/R = 2$ and velocity of 20m/sec. The movements in Fig.19 are in the mixed form of steady and unsteady vibration and rotation in which at low initial object angle of attack, as a result of perpendicular force to the plates, the movement is rotational; at initial object angle of attack of 16 and 24 degrees, it is unsteady vibrational; and at higher than 32 degrees, it is steady rotational around the angle of 45 degrees.

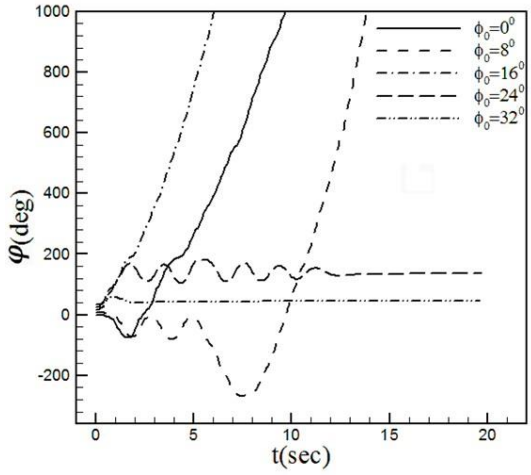

Fig. 15 Variation of object angle with time for cylinder with a length of 24cm, length ratio of 3 and free stream velocity of 8m/sec

In Fig. 15, the angular changes of cylinder with length of 24cm, $L/R = 3$ and velocity of 8m/sec has been shown. As the initial object angle of attack increases to 45 degrees, the movement regime changes from steady to unsteady rotation and then to steady vibrations (at initial object angle of 32 degrees) due to the reduced perpendicular force to the plates.

When the cylinder length increases to 24cm and$L/R = 1$, the rotational movement regime appears at free stream velocity of 30m/sec and low initial object angle of attack; while for a cylinder of 16cm length and $L/R = 1$, the movement regime at all velocities is vibrational. In other words, it can be said that as the cylinder length increases to 24cm, the three dimensional effects of the flow disappear and the moment induced to the plates goes up.

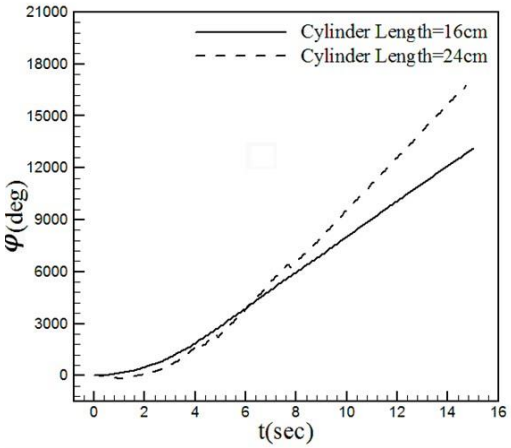

Fig. 16 Variation of object angle with time for different cylinder lengths on length ratio of 3 and free stream velocity of 15m/sec

Figure 16 clearly indicates the result for an$L/R = 3$ and velocity of 13m/sec. It is obvious that with the increase of cylinder length, the angular velocity of the model, resulting from the increased force induced to the plates, has gone up.

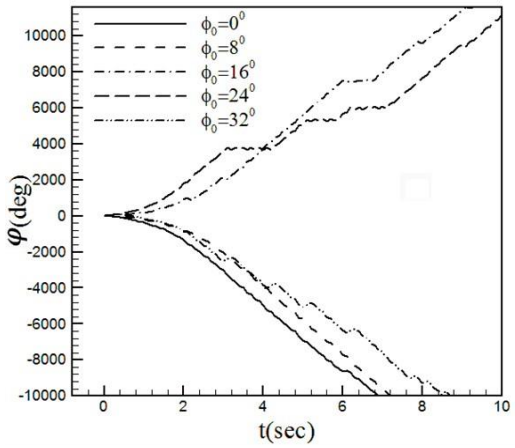

Fig. 17 Variation of object angle with time for cylinder with a length of 24cm, length ratio of 3 and free stream velocity of 15m/sec

Figure 17 illustrates the steady rotational movement of a cylinder with the length of 24cm, $L/R = 3$ and free stream velocity of 5m/sec at different angles of attack.

The non-dimensional Strouhal number represents the flow vibration that is attained by$S_t = \frac{fl}{V}$, in which f is the frequency, $l$as the length and$V$as the free stream velocity. Sarpkaya asserted that when the amplitude of the body vibrations intensifies, the frequency of flow vibration becomes equal to the body rotational/ vibrational frequency. As a result, instead of flow vibrations, body rotational frequency was used to calculate Strouhal number.

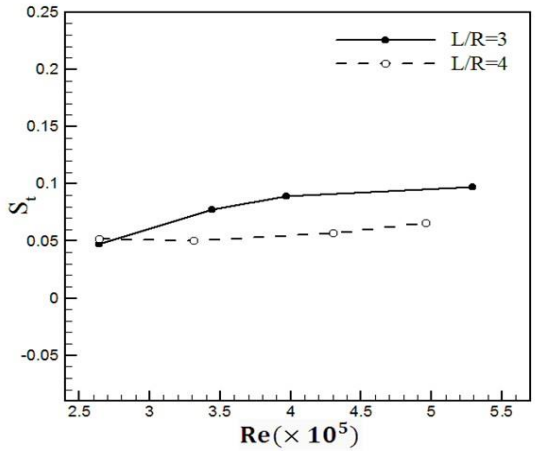

Fig. 18 Variation of Strouhal number with Reynolds number for cylinder with a length of 24cmand four plates

Figure 18 displays the alterations of Strouhal number compared to Reynolds number for a cylinder of four plates of 16cm length, and $L/R = 3$ and$L/R = 4$. The findings have revealed that as the Reynolds number increases, Strouhal number remains fixed. Bloyens also shows that for a rotating cylinder, Strouhal number alterations as compared to Reynolds number, has a fixed value of 0.2. The average Strouhal number for $L/R = 3$ is 0.0795 and for $L/R = 4$ is 0.0549.

Comparison of Experimental and Numerical Result

Figure 19 compares the experimental and numerical results for an object angle changes during time for $L/R = 2$, free stream velocity of 13m/sec and initial object angle of 32 degrees. The movement regime is rotational at the equilibrium angle of 45 degrees. In the experimental procedure, the effects of three dimensional flow that causes the body vibrations in comparison with the numerical procedure has a lower amplitude, that is, other vibrations of the body have more damping.

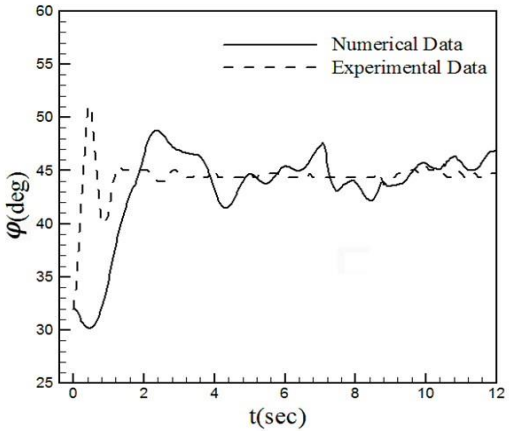

Fig. 19 Comparison between experimental and numerical data for variation of object angle with time for a length ratio of 2 and initial object angle of attack of 32 degrees and free stream velocity of 13m/sec

Figure 20 compares the numerical and experimental results of the object angle changes during time for $L/R = 2$, free stream velocity of 20m/sec and initial object angle of attack of 8 degrees. As can be seen, during the whole time, the movement in both experimental and numerical is steady rotational. Initially, the rotational angular velocity in the experimental procedure was more than the numerical one. But as time passed, the angular velocity became less than that of numerical one, causing damping as a result of the effects of 3-D flow.

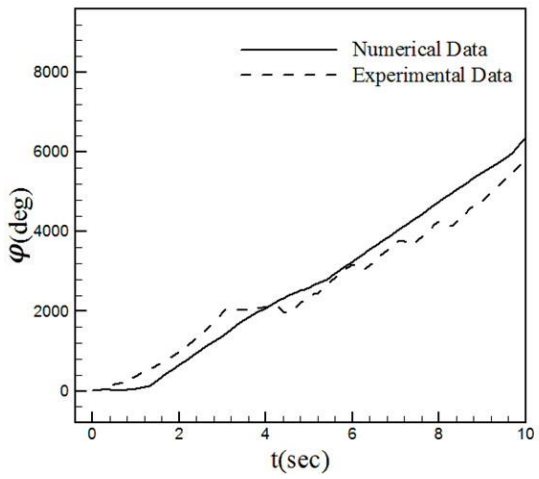

Fig. 20 Comparison between experimental and numerical data for variation of object angle with time for a length ratio of 2 and initial object angle of attack of 8 degrees and free stream velocity of 20m/sec

Conclusion

In the present research, the dynamic behaviors of a cylinder with four plates attached to it in the unsteady flow, via both experimental and numerical procedure known as discrete vortex, were modeled and analyzed. The results report that the model in the steady flow with different L/R, velocities and initial object angles of attack showed varied movement patterns including steady rotation, unsteady rotation, steady vibration and unsteady vibration. This can be attributed to the force induced from the flow to the body. When there is such a force from the flow on the body, the aerodynamic damping is negative.

The numerical results showed that the vortex shedding pattern from the plate edges to downstream in the steady vibrational movements is as 2S; but, in the rotational movement, vortices irregularity separate from the plate edges and move downstream. In the steady vibrational movement, the vortex distribution in each cycle near the two plates at equilibrium angle (45 degrees) is symmetrical, which leads to lower moment induced to the plates and reduced angular velocity. Such a velocity reduction and moment around 45 degrees were also obtained from vibrational movement in experimental procedure by contrast, in the rotational movement regime, the vortex distribution around the four plates was always asymmetrical; consequently, the moment and perpendicular force induced to the plates intermittently and irregularly changed. In both experimental and numerical procedures, it was seen that the angular velocity after the release in free flow had increased and, after a definite time on, it irregularly vibrated at a fixed value. It has also been shown that rotational movement regime, in both numerical and experimental procedures at a fixed L/R and fee stream velocity, is created at low initial object angle of attack. When the initial object angle of attack increases to the equilibrium angle of 45 degrees, the movement changes to steady vibrational one. As L/R increases, the initial object angle of attack in vibrational movement increases in a way that $L/R = 4$. All the initial object angles of attack are as steady rotational ones. This causes increase of the area perpendicular to the flow, more forces induced to the plates and change to rotational movement. The minimum Strouhal number is calculated at different $L/R$is 0.0275 for rotational movements. Also, as the Reynolds number increases, the Strouhal number remains fixed. This fixed values for $L/R = 3$and $L/R = 4$are 0.0795 and 0.0549, respectively.

Reference

[1]Van Dyke, M.,(1982). *An Album of Fluid Motion*, 10th Edition. Parabolic Press,Stanford, CA, USA.

[2] Feng, C. C.,(1968). The measurement of vortex induced effects in flow past stationary and oscillating circular and d-section cylinders,(Master's Thesis), The University of British Columbia, Canada.

[3] Amandolese, X., Hemon, P.,(2010). "Vortex-induced vibration of a square cylinder in wind tunnel,"*Comptes Rendus Mecanique 338*, pp. 12-17.

[4]Umemura, S., Yamaguchi, T., Shiraki, K.(1971). "On the vibration of Cylinders caused by Karman Vortex,"*Bulletin of Japan Society of Mechanical Engineering*, Vol.14, No.75, pp.929-936, 1971.

[5] Sarpkaya, T.,(1979). "Vortex-induced vibrations, a selective review."*Journal of Applied Mechanics*, Vol.46, No.2, pp.241-258.

[6] Sarpkaya, T.,(2004). "A critical review of the intrinsic nature of vortex induced vibration,"*Journal of Fluids and Structures*, Vol. 19(4), pp. 389-447.

[7] Scanlan, R. H., Rosenbaum, R.,(1968). *Aircraft vibration and flutter*. Dover, New York, USA.

[8] Protos, A., Goldschmidt, V. W., Toebes, G. H.,(1968). "Hydroelastic forces on bluff cylinders."*ASME Journal of Basic Engineering*, Vol.90, No.3, pp.378-386.

[9] Bearman, P. W. ,Obasaju, E. D.,(1982). An experimental study of pressure fluctuations on fixed and oscillating Square-Section cylinders. *Journal of Fluid Mechanics*, Vol.119, pp.297–321.

[10]Williamson, C. H. K., Roshko, A.,(1988), "Vortex formation in the wake of an oscillating cylinder,"*Journal of Fluids and Structures*, Vol. 2(4), pp.355-381.

[11]Griffin, O. M., Skop,R. A., Ramberg,S. E.,(1976). "Modeling of the vortex-induced oscillations of cables and bluff structures,"*Society for Experimental Stress Analysis Spring Meeting*, Silver Spring, MD, USA.

[12]Kiya, M., Arie, M.,(1980). "Discrete-vortex simulation of unsteady separated flow behind a nearly normal plate."*Bulletin of Japan Society of Mechanical Engineering*, Vol. 23, No.183, pp. 1451-1458.

[13]Isvand, H.,(2002). Numerical and experimental investigation of free rotational and oscillations of body in air flow,(PhD Thesis), Mosco State University, Russia.